AN IMPROVED PIXON-BASED APPROACH FOR IMAGE SEGMENTATION

H. Hassanpour*

School of Computer Engineering & IT, Shahrood University of Technology
Shahrood, Iran, h_hassanpour@yahoo.com

H. Yousefian

Department of Electrical Engineering, Iran University of of Science and Technology (IUST)
Tehran, Iran, hadi_yousefian18@yahoo.com

*Corresponding Author

(Received: June 29, 2009 – Accepted in Revised Form: March 11, 2010)

Abstract An improved pixon-based method is proposed in this paper for image segmentation. In this approach, a wavelet thresholding technique is initially applied on the image to reduce noise and to slightly smooth the image. This technique causes an image not to be oversegmented when the pixon-based method is used. Indeed, the wavelet thresholding, as a pre-processing step, eliminates the unnecessary details of the image and results in a fewer pixon number, faster performance and more robustness against unwanted environmental noises. The image is then considered as a pixonal model with a new structure. The obtained image is segmented using the hierarchical clustering method (Fuzzy C-Means algorithm). The experimental results in this paper indicate that the proposed pixon-based approach has a reduced computational load and a better accuracy compared to the other existing image segmentation techniques.

Keywords Image segmentation, Pixon, Wavelet thresholding

چکیده [illegible] (C-Means [illegible]

1. INTRODUCTION

Image segmentation is a process of partitioning image into several disjoint regions with similar characteristics in terms of intensity, color and texture. It has wide applications in image processing and is often employed as a pre-processing stage in various applications such as mobile object tracking, medical imaging and face recognition [1].

A considerable number of segmentation techniques exist in the literature. These techniques can be classified in several groups; thresholding-based methods, which determine threshold values using the image histogram and then classify the image pixels based on these values [2]; region-based methods, which group pixels into homogeneous regions and segment the image to some major areas, such as region growing [3, 4]; clustering-based methods, which segment the feature space of image to several clusters and get a sketch of the original image, such as K-means [5], Fuzzy C-Means (FCM) [6] and mean-shift [7] algorithms. Modeling images with Markov Random Fields (MRF) is another approach which has been recently developed to segment images [8-10]. To achieve this purpose, these methods try to minimize the energy function of image using clique concept and Gibbs distribution. However, the main disadvantage of MRF-based methods is

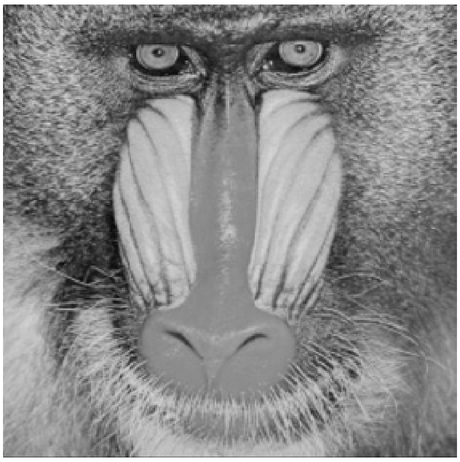

(a)

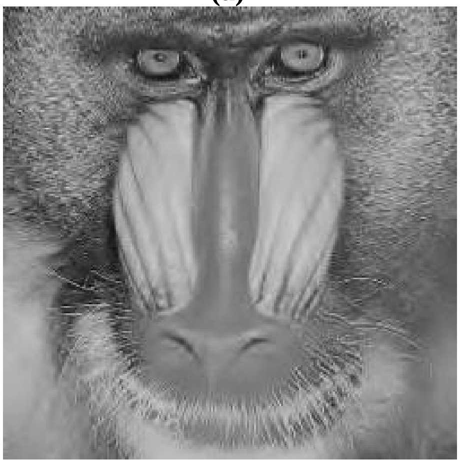

(b)

Figure 2. Result of applying wavelet thresholding technique on Baboon image: (a) Original image, and (b) smoothed image.

The output of pre-processing step is then used in the pixon formulation stage. In Yang's pixon-based algorithm, after obtaining the pseudo image, the anisotropic diffusion equation was used to form the pixons. In our proposed algorithm, utilizing the wavelet thresholding method as a pre-processing stage eliminates the necessity of using the diffusion equations. After forming and extracting the pixons, the Fuzzy C-Means (FCM) algorithm is used to segment the image. The FCM algorithm is an iterative procedure described in the following [20]:

Given M input data $\{x_m; m = 1, \ldots, M\}$, the number of clusters C $(2 \leq C < M)$, and the fuzzy weighting exponent w, $1 < w < \infty$, initialize the fuzzy membership functions $u^{(0)}{}_{c,m}$ with $c = 1, \ldots, C$ and $m = 1, \ldots, M$ which are the entry of

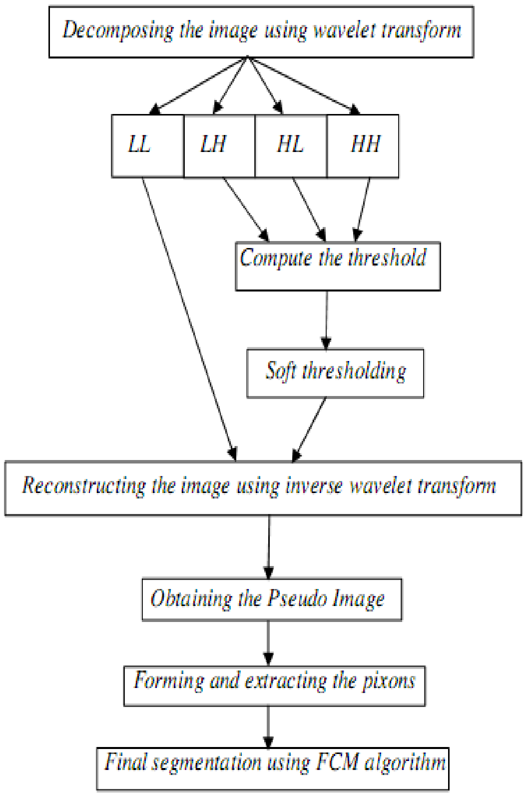

Figure 3. The block diagram of the proposed method.

a $C \times M$ matrix $U^{(0)}$. The following procedure is performed for iteration $l = 1,2, \ldots$:

1. Calculate the fuzzy cluster centers $v_c{}^l$ using $v_c = \sum_{m=1}^{M} (u_{c,m})^w x_m \,/\, \sum_{m=1}^{M} (u_{c,m})^w$.

2. Update $U^{(l)}$ using $u_{c,m} = 1/\sum_{i=1}^{C} (\frac{d_{c,m}}{d_{i,m}})^{\frac{2}{w-1}}$ where $(d_{i,m})^2 = \|x_m - v_i\|^2$ and $\|\,.\,\|$ is an inner product induced norm.

3. Compare $U^{(l)}$ with $U^{(l+1)}$ in a convenient matrix norm. If $\left\|U^{(l+1)} - U^{(l)}\right\| \leq \varepsilon$ stop; otherwise continue from step 1.

The value of the weighting exponent, *w* determines the fuzziness of the clustering decision. A smaller value of *w*, i.e. *w* is close to unity, will give the zero/one hard decision membership function, and a larger *w* corresponds to a fuzzier output. Our experimental results suggest that *w* = 2 is a good choice.

Figure 3 illustrates the proposed method block diagram.

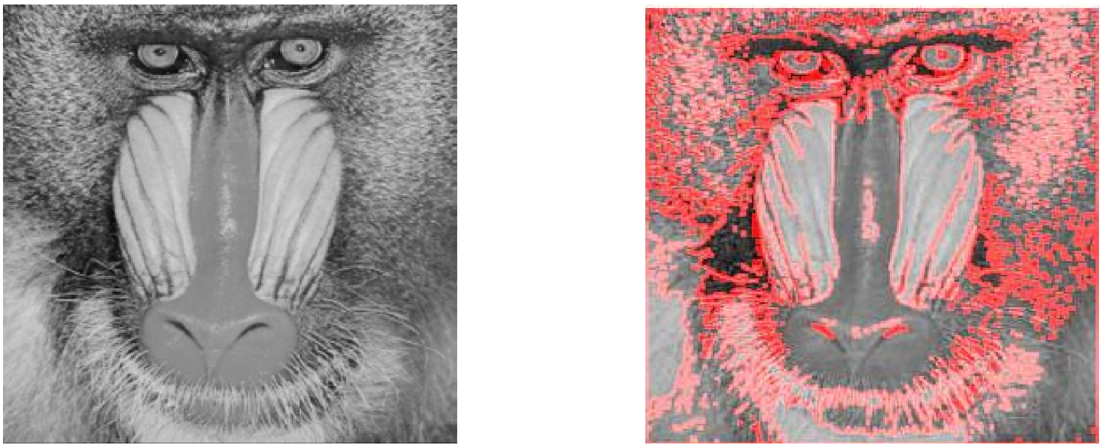

(a) (b)

Figure 4. The effect of applying the pixon forming algorithm to the Baboon image: (a) the original image, (b) the output image with boundaries between pixons.

4. EXPERIMENTAL RESULTS

In this section, first we indicate the effect of pixon forming stage on an arbitrary image. As illustrated in Fig. 4, the boundaries between the adjacent pixons are sketched so that the image segments are more proper.

The proposed segmentation method is applied on several standard images and the results of these implementations are extracted. In this section, the commonly used images such as Cortex, Baboon, and Pepper are selected and the performance of applying the proposed method on them is compared with those of two other existing approaches; Yang's method [13] and Lin's method [14]. Figs. 5(a), 6(a) and 7(a) are the Baboon, Pepper and Cortex images used in our experiment. Figs. 5(b), 6(b), 7(b) and 5(c), 6(c), 7(c) show the segmentation results of Yang's and Lin's methods, respectively. The segmentation results of our approach are illustrated in Figs. 5(d), 6(d) and 7(d). As shown in these figures, the homogeneity of regions and the discontinuity between adjacent regions, which are two main criteria in image segmentation, are enhanced in the results associated with the proposed method. In addition, several experiments have been carried out on different images and the average results are drawn in several tables. As can be seen from Table 1, the number of pixons and consequently the ratio of Pixon-Pixel in the proposed approach are decreased significantly. This is the result of applying the wavelet thresholding technique before forming pixons.

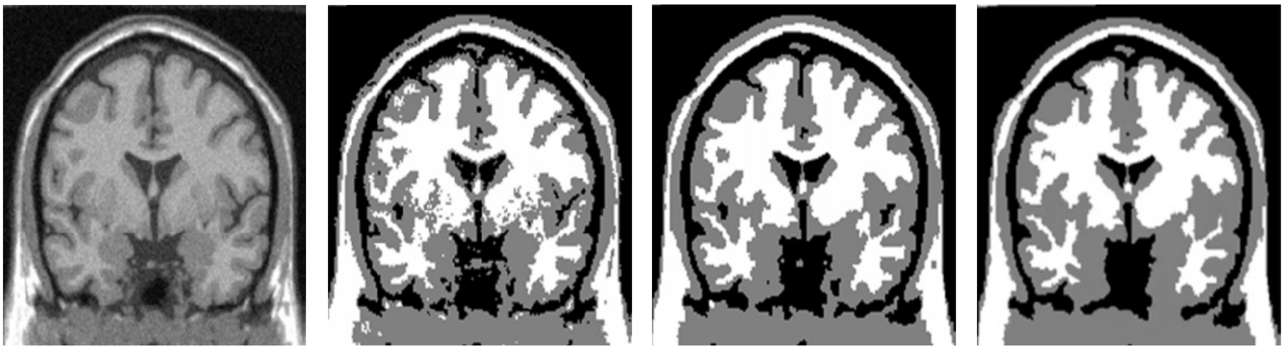

(a) (b) (c) (d)

Figure 5. Segmentation results of the Cortex image: (a) Original image, (b) Yang's method, (c) Lin's method, and (d) proposed approach.

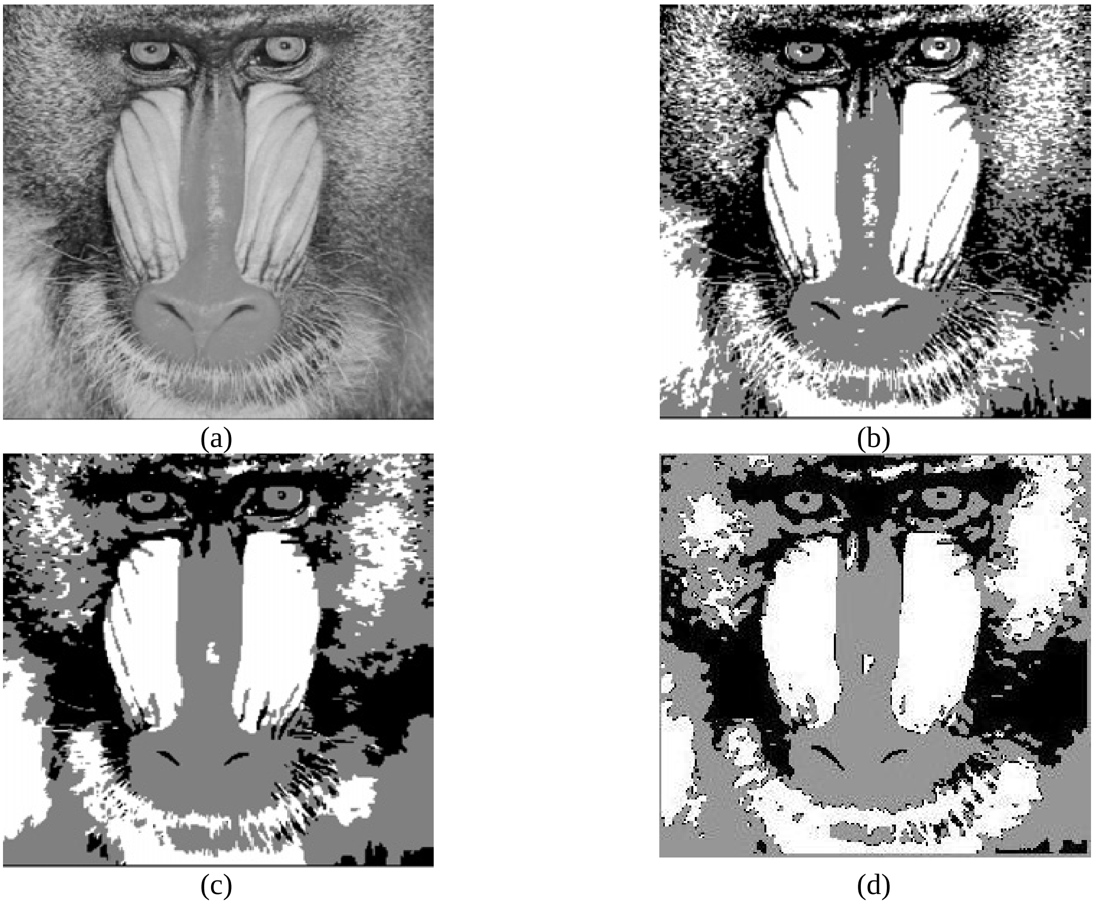

Figure 6. Segmentation results of the Baboon image: (a) Original image, (b) Yang's method, (c) Lin's method, and (d) proposed approach.

Table 2 shows the computational time required for the three methods (*computer specifications:* Intel(R) Core(TM)2 Duo CPU 2.20 GHz processor, using MATLAB 7.4). By using pixon concept with wavelet thresholding technique in our approach, the computational cost is sharply reduced. One of the most important parameters used to evaluate the performance of image segmentation methods is the variance of each segment. The smaller value of this parameter implies the more homogeneity of the region and consequently the better segmentation results. In this paper, after the segmentation process, the images are divided into three segments with possibly different average values. We have called these segments as "Classes". The variance and average of each class associated with the above-mentioned images are listed in Tables 3-5. As can be inferred from the results, the variance values for the majority of classes from different images in our method are smaller in comparison to those from the other methods. In addition to the typical variance, we calculate the normalized variance of each image after applying the three above-mentioned image segmentation approaches. If N_k and $V(k)$ denote the number of the pixels and the variance of each class respectively, the normalized variance of each image can be determined as below:

$$V^* = \frac{V_N}{V_l} \tag{7}$$

where

$$V_N = \sum_{k=1}^{K} \frac{N_k V_k}{N} \tag{8}$$

and

$$V_l = \sum_{k=1}^{K} \frac{(I(x,y) - M)^2}{N} \tag{9}$$

In the above equations, k denotes the number of

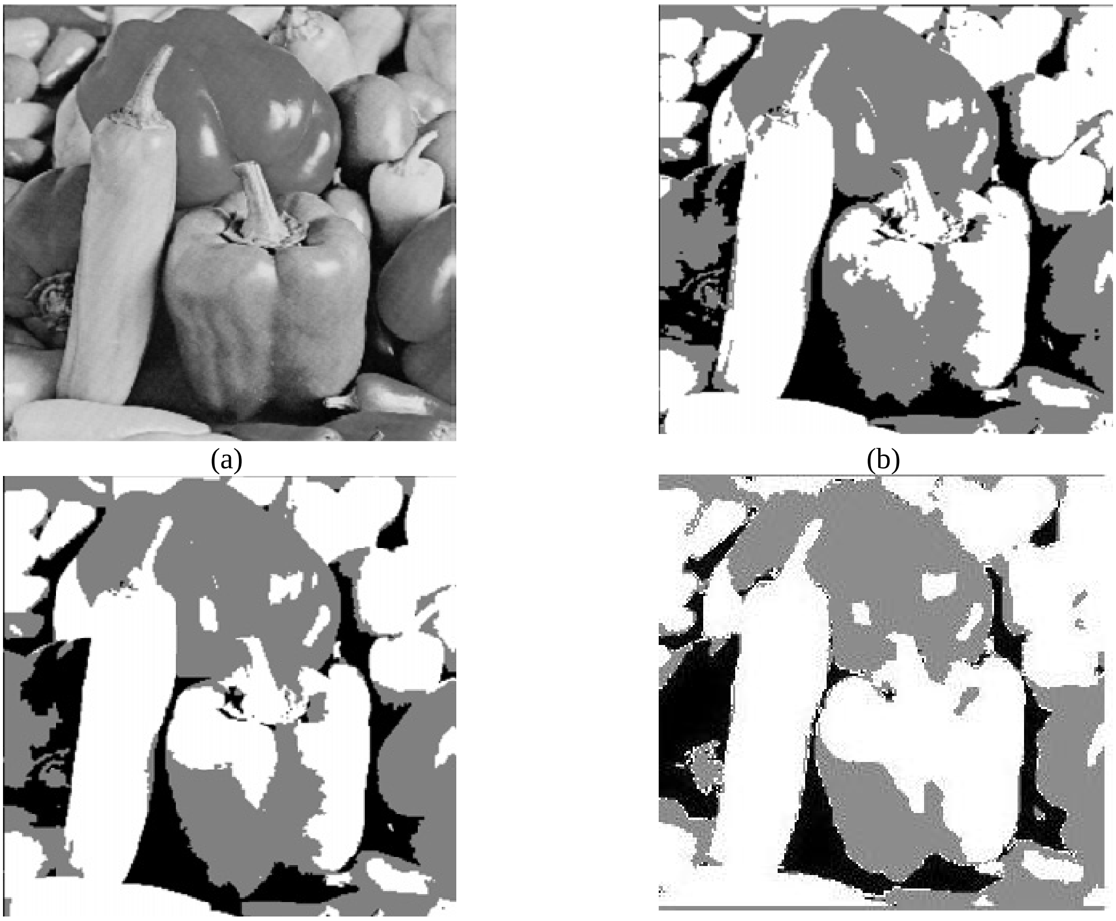

Figure 7. Segmentation results of the Pepper image: (a) Original image, (b) Yang's method, (c) Lin's method, and (d) proposed approach.

classes, $I(x, y)$ is the gray level intensity, M and N are the averaged value and the number of pixels in each image respectively. The normalized variance results illustrated in the tables demonstrate that in our approach, the amount of pixels in each cluster is closer to each other and the areas of images are more homogenous. Consequently, as can be inferred clearly from the figures, the proposed method shows a better performance in image segmentation compared to the other methods.

5. CONCLUSIONS

We have proposed an improved pixon-based method for image segmentation with utilizing the wavelet thresholding technique as a pre-processing step. Both the smoothness and uniformity of the obtained image are increased compared to the original image by using the pre-processing step. In addition, the SNR value is improved in the obtained image as the wavelet thresholding is an effective method in noise reduction. Then the pixon-representation of the image has been extracted and the Fuzzy C-Means (FCM) algorithm is successfully used to segment the image. By incorporating the pixon concept and wavelet thresholding into our method, a considerable decrement in computational costs has been achieved. If the size of image is increased, the quality of the results associated with the proposed method may not change. But the computational time of the algorithm will be certainly increased. The gained results indicate that in our technique the criteria are greatly enhanced compared to the two other well known methods and good segmentation results are obtained.

Table.1. Comparison of the number of pixons and the ratio between the number of pixons and pixels, among the three methods.

Images (Size)	The number of pixels	The number of pixons			The ratio between the number of pixons and pixels		
		Yang's method	Lin's method	Proposed method	Yang's method	Lin's method	Proposed method
Baboon (256×256)	262144	83362	61341	25652	31.8 %	23.4 %	9.79 %
Pepper (256×256)	262144	31981	24720	13221	12.2 %	9.43 %	5.04 %
Cortex (128×128)	16384	1819	1687	1523	11.1 %	10.2 %	9.3 %

Table.2. Comparison of the computational time, between the three methods.

Images	Yang's method (ms)	Lin's method (ms)	Proposed method(ms)
Baboon	18549	19326	15316
Pepper	16143	17034	13066
Cortex	712	697	633

Table.3. Comparison of variance values of each class, for the three algorithms (Baboon).

Method	Parameter	class 1	class 2	class 3
Yang's method	average	168.06	127.28	84.25
	variance	12.18	11.06	17.36
	Normalized Variance	**0.0279**		
Lin's method	average	167.86	126.45	82.18
	variance	12.05	11.55	16.67
	Normalized Variance	**0.0259**		
Proposed method	average	170.40	128.36	83.95
	variance	11.34	11.46	16.96
	Normalized Variance	**0.0212**		

Table.4. Comparison of variance values of each class, for the three algorithms (Pepper).

Method	Parameter	class 1	class 2	class 3
Yang's method	average	190.59	123.29	35.47
	variance	16.64	21.89	21.79
	Normalized Variance	**0.0263**		
Lin's method	average	191.68	125.27	34.39
	variance	16.28	22.66	22.30
	Normalized Variance	**0.0251**		
Proposed method	average	189.75	122.56	37.17
	variance	15.87	22.86	20.30
	Normalized Variance	**0.0217**		

Table.5. Comparison of variance values of each class, for the three algorithms. (Cortex)

Method	Parameter	class 1	class 2	class 3
Yang's method	average	22.44	93.71	197.23
	variance	12.59	11.67	14.11
	Normalized Variance	**0.0131**		
Lin's method	average	21.34	91.65	199.50
	variance	12.75	10.33	13.93
	Normalized Variance	**0.0119**		
Proposed method	average	24.25	92.49	196.72
	variance	11.37	10.51	12.81
	Normalized Variance	**0.0101**		

6. REFERENCES

1. Gonzalez, R.C. and Woods, R.E., “Digital Image Processing**”**, Prentice Hall, (2004).
2. Bonnet, N., Cutrona, J., and Herbin, M., “A ‘no-threshold’ histogram-based image segmentation method”, ***Pattern Recognition***, Vol. 35, Issue 10, (2002), 2319-2322.
3. Shi, J. and Malik, J., “Normalized cuts and image segmentation”, ***IEEE Trans. Pattern Anal. Mach. Intell.*** , Vol. 22, No 8, (2000), 888–905.
4. Zhu, S.C. and Yuille, A., “Region competition: unifying snakes, region growing, and byes/mdl for multi-band image segmentation”, ***IEEE Trans. Pattern Anal.***

Mach. Intell., Vol. 18, No 9, (1996), 884–900.
5. Papamichail, G. P. and Papamichail, D.P., "The k-means range algorithm for personalized data clustering in e-commerce", ***European Journal of Operational Research***, Vol. 177, Issue 3, (2007), 1400-1408.
6. De Carvalho, F.A.T., "Fuzzy c-means clustering methods for symbolic interval data", ***Pattern Recognition Letters***, Vol. 28, Issue 4, (2007), 423-437.
7. Comaniciu, D. and Meer, P., "Mean shift: a robust approach toward feature space analysis***", IEEE Trans. Pattern Anal. Mach. Intell***., Vol. 24, No. 5, (2002), 1–18.
8. Lakshmanan, S. and Derin, H, "Simultaneous parameter estimation and segmentation of Gibbs random fields using simulated annealing", ***IEEE Trans. Pattern Anal. Machine Intell.***, Vol. 11, No. 8, (1989), 799–813.
9. Kato, Z., Zerubia, J., and Berthod, M., "Unsupervised parallel image classification using Markovian models", ***Pattern Recogniion***, Vol. 32, (1999), 591–604.
10. Elfadel, I.M. and Picard, R.W., "Gibbs random fields, cooccurrences, and texture modeling", ***IEEE Trans. Pattern Anal. Machine Intell.***,Vol. 16,(1994), 24–37.
11. Piña, R.K. and Pueter, R.C., "Bayesian image reconstruction: The pixon and optimal image modeling", ***P. A. S. P.,*** Vol. 105, (1993), 630–637.
12. Puetter, R.C., "Pixon-based multiresolution image reconstruction and the quantification of picture information content", ***Int. J. Imag. Syst. Technol***., Vol. 6, (1995), 314–331.
13. Yang, F. and Jiang, T., "Pixon-based image segmentation with Markov random fields", ***IEEE Trans. Image Process***., Vol. 12, No. 12, (2003), 1552–1559.
14. Lin, L., Zhu, L., Yang, F., and Jiang, T., "A novel pixon-representation for image segmentation based on Markov random field", ***Image and Vision Computing,*** Vol. 26, (2008), 1507–1514.
15. Donoho, D. L. and Johnstone, I.M., "Ideal spatial adaptation via wavelet shrinkage", ***Biometrika***, Vol. 81, (1994), 425-455.
16. Jansen, M., "Noise Reduction by Wavelet Thresholding", Springer Verlag New York Inc., (2001).
17. Chang, S.G., Yu, B. and Vetterli, M., "Adaptive Wavelet Thresholding for image Denoising and compression", ***IEEE Trans. Image Processing***, Vol.9, No.9, (2000), 1532-1545.
18. Gupta, S. and Kaur, L., "Wavelet Based Image Compression using Daubechies Filters", ***In proc. 8th National Conference on Communications,*** I.I.T. Bombay, (2002).
19. Burrus, C.S., Gopinath, R. A., and Guo, H., "Introduction to Wavelets and Wavelet Transforms: A Primer", New Jersey: Prentice Hall, (1998).
20. Fauzi, M.F.A. and Lewis, P.H., "A Fully Unsupervised Texture Segmentation Algorithm", ***British Machine Vision Conference***, Norwich, UK. (2003).